Simple Nd:YAG laser generates vector and vortex beam

Zhiqiang Fang (方志强), Yao Yao (姚 瑶), Kegui Xia (夏克贵), and Jianlang Li (李建郎)*

Shanghai Institute of Optics and Fine Mechanics, Chinese Academy of Sciences, Shanghai 201800, China

**Corresponding author: apuli@siom.ac.cn*

Received October 31, 2014; accepted January 16, 2015; posted online February 24, 2015

We report a simple Nd:YAG laser that emits radially polarized beam with helical wavefront. The laser cavity consists of a piece of laser crystal and a plane output coupler, and there is no additional polarization component inside it. The pump light is converted into annular profile through de-focal coupling into a multi-mode fiber. For the continuous-wave (CW) operation, the laser emits radially polarized vortex beam, and it is observed that the helical wavefront of the laser beam is switched from right handedness to left handedness when the output coupler is tilted slightly. For the Q-switched operation under the insertion of a Cr^{4+}:YAG saturable absorber inside the cavity, we obtain radially polarized outputs with left-handedness helical wavefront. By tilting the laser crystal slightly, the laser output switches to azimuthal polarization at pump power larger than 4.5 W and left-handedness helical wavefront of laser beam is preserved.

OCIS codes: 140.3580, 140.3540, 140.3530, 140.3480, 140.3410.

doi: 10.3788/COL201513.031405.

Optical singularities have drawn much interest recently[1,2]. These singularities occur at points or lines where the phase or the polarization of field is undefined or changes abruptly. Past researches were devoted to phase singularities in homogeneously polarized light waves, especially the scalar vortex. Scalar vortex, which has a spiral phase wavefront with a central singularity point where the phase is undefined, has become a fashionable topic in optical physics, partly through their relationship with beams carrying orbital angular momentum (OAM)[3]. To generate such beams carrying OAM, many techniques had been proposed[4–7].

Phase singularities are features of scalar optics and occur naturally only in scalar components of vector fields. In fields where the state of polarization varies with position, polarization singularities can occur. One special case, the radially polarized beam is of special interest because it can produce very small focal spots or generate longitudinal electric field components upon focalization[8]. Due to the important applications in many fields, the generation of vector beams has attracted lots of interests in recent years[9–14].

In recent years, the vector vortex beam, especially the radially polarized vortex beam, where the polarization singularity is also a phase singularity, have received particular attention owing to their possessing of tight focusing and OAM[15–17]. Those beams have been proved to be useful in many fields such as particle trapping and manipulation[18–20], surface plasmon polaritons excitation[21], material processing[22] and etc. Several methods have been proposed for the generation of vector-vortex beam. The method based on subwavelength metallic and dielectric gratings had been proposed for several years[21–24]. A nanostructure glass converter created by femtosecond direct-writing technology had been used to form radially polarized vortex beam recently[25]. We also realized the formation of vector-vortex beam in a few-mode fiber[26].

The above-mentioned methods focused on the passive way to achieve vector vortex laser beam, and they did not refer to active resonator. In this Letter, we demonstrated a Nd:YAG laser that emitted radially polarized LG_{01} mode beam with helical wavefront. For the continuous-wave (CW) operation, we obtained spiral phase structure with right handedness. By slightly tilting the output coupler (OC), the helical wavefront was transformed to left handedness. When the laser was operated in Q-switched mode, we obtained both radially and azimuthally polarized laser modes accompanied by spiral phase wavefront with left handedness. More details are described as follows.

Figure 1 shows the schematic diagram of the experimental setup of CW Nd:YAG laser, which consists of only laser crystal, OC, and annular pump light. The Nd:YAG laser crystal was doped with 1.0 at.% neodymium ion concentration, and it had the dimensions of 10 mm in diameter and 2 mm in thickness. A planar mirror with 2% transmittance at 1064 nm was deployed as an OC. The total length of laser cavity was 11 cm. By slightly adjusting the distance between lens L_2 and multi-mode optical fiber, the pump light from an 808 nm laser diode (LD) was reshaped into annular intensity distribution, and then was delivered into the plano–plano laser cavity. With such arrangement, an efficient LG_{01} mode output was obtained and also the output was radially polarized. This laser gave a maximum output power of 1.2 W at 1064 nm with a slope efficiency of 28.3% in the name of incident pump power. Figures 2(a) and 2(b) depict the far- and near-field full beam profiles at 3.2 W incident pump power. The polarization states of the laser mode were checked by applying a linear polarizer analyzer. The images in Figs. 2(c)–2(f) plot the corresponding far-field intensity distribution of laser beam transmitted through the linear polarizer analyzer. As seen in the pictures, the symmetric two-lobe patterns were always parallel to the corresponding directions of the linear polarizer's axis, and this phenomenon manifested

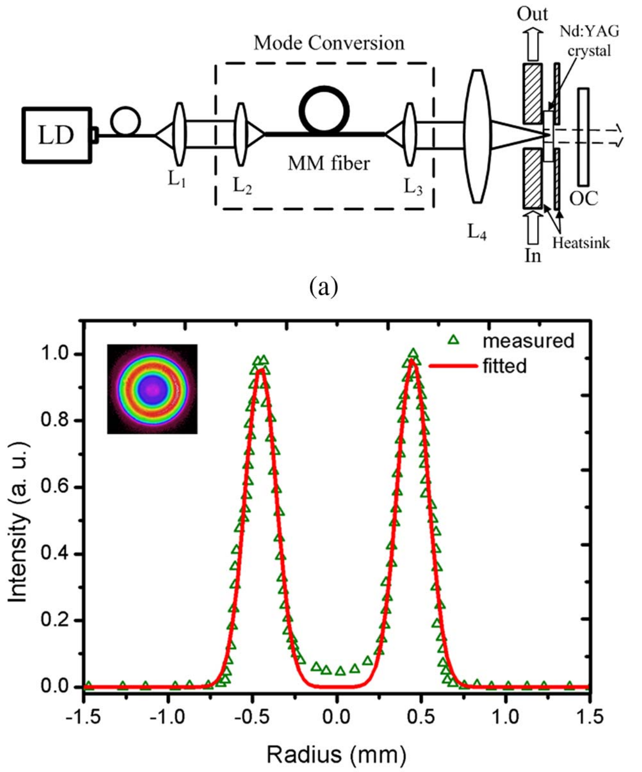

Fig. 1. (a) Schematic diagram of CW Nd:YAG laser by using annular pumping, and (b) captured intensity distribution of pumping light at L_4's focal plane by applying 90 μm off-focus coupling.

the doughnut-shaped laser beam were radially polarized. The degree of polarization of the beam was also measured to be 83.3%. The results mentioned in this section had been described in our recent works[27] and readers can refer to it for more details.

The phase structure of laser beam was measured by the interference between itself and a spherical reference wave in a Mach–Zehnder interferometer. Figure 3(a) shows the applied interferometer schematically. The output beam from the laser cavity was expanded by a beam expander (BE) with a pair of lenses, and then was divided into two beams by a non-polarizing beam splitter (NPBS). The beam in the upper arm was used as the probe wave and was clipped by a small aperture before becoming a spherical wave by a lens. The beam in the lower arm acted as signal wave and interfered with the probe beam in front of a CCD camera. Figure 3(b) shows the captured interference patterns and the spiral structure of it strongly suggests that the laser beam was a pure LG_{01} mode with a phase dependence of $\exp(i\phi)$, namely, a topological charge of +1. By slight tilting the laser's OC while keeping both the intensity and polarization of laser beam unchanged, the spiral structure of interference pattern became counterclockwise as shown in Fig. 3(c), and this suggested that a phase factor of $\exp(-i\phi)$ was incorporated and showed the left handedness of the laser beam. The mechanism for the handedness switching by tilting the OC was not yet understood at this moment and hence it would be the subject of ongoing investigation.

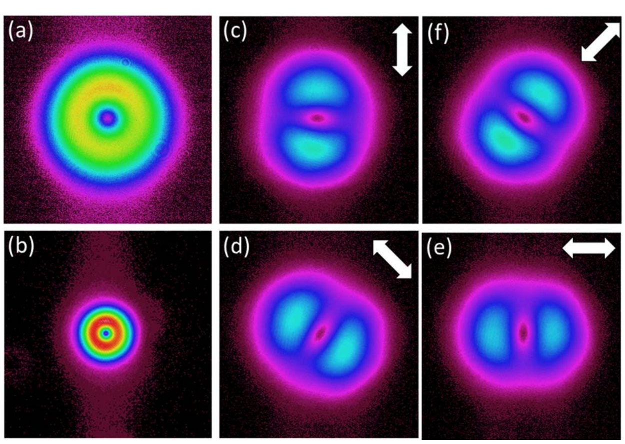

Fig. 2. (a) Far- and (b) near-field intensity distributions of the laser beam at 3.2 W pump power for CW Nd:YAG laser; (c)–(f) far-field intensity profiles of laser beam transmitted through the polarizer analyzer. The white arrows indicate the respective orientations of the polarizer analyzer's axis.

Further, we also demonstrated passively Q-switched operation of this Nd:YAG laser by inserting a Cr^{4+}:YAG saturable absorber (SA) into the laser cavity, and obtained the stable and reproducible Q-switched oscillation. At this time, the lens L_4 had a focal length of 15 mm, and the initial transmission of SA was 90%. Further, the length of laser cavity was shortened to 8 cm and. With such arrangement, the slope efficiency of laser was about 32%, and the laser pulse had 3.3 kW peak power, 39 ns pulse duration at 2.5 kHz repetition rate. Figures 4(a) and 4(b) show an example of the measured far- and near-field intensity distributions of obtained laser beam at 3.8 W absorbed pump power. Such doughnut-shaped laser beam was always radially polarized in the whole range of pump power above the lasing threshold. Figures 4(c)–4(f) depicts the corresponding far-field intensity distribution of the transmitted beam through a polarizer analyzer at different directions of polarizer's axis, and these images served as the evidence of radially polarized laser oscillation. The above-mentioned results had been given in one of our recent works[28] and readers can refer to it for more details.

Further, the pulsed laser output was delivered into the interferometer plotted in Fig. 3, and the interference pattern as plotted in Fig. 4(g) showed a counterclockwise spiral structure, and the left handedness of this pattern indicated the topological charge of the laser beam was −1.

Based on the same arrangement of above-described passively Q-switched laser, we tilted the laser crystal slightly and observed that polarization state of laser beam was switched to azimuthal polarization at high pump power beyond 4.5 W. Such polarization-switching phenomenon above a critical pump power of 4.5 W was reproducible, and can be interpreted as the overlap efficiency of the azimuthally polarized component with annular pump field exceeded that of radially polarized component when the

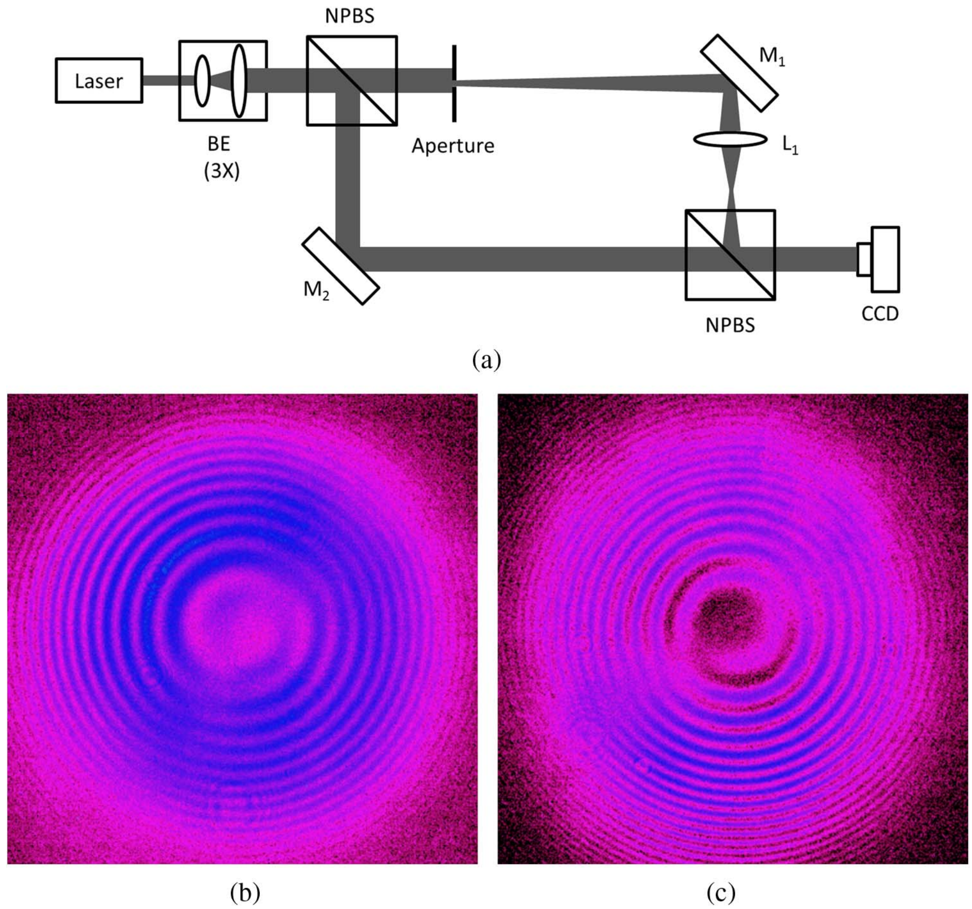

Fig. 3. (a) Experimental setup of Mach–Zehnder interferometer and spiral interference patterns with (b) right handedness and (c) left handedness at an incident pump power of 3.2 W. M_1, M_2, flat mirror with high reflectivity; L_1, lens with $f = 40$ mm.

laser crystal was tilted slightly[28]. Figures 5(a) and 5(b) plot the captured far- and near-field full beam profiles at 4.9 W absorbed pump power. Figures 5(c)–5(f) plot the transmitted two-lobe structures at different orientations of polarizer's axis, in which the null line of each two-lobe structure is always parallel to the corresponding polarizer's axis. This verified the laser beam was azimuthally polarized.

The phase structure of the azimuthally polarized laser beam was also measured by interference. We delivered laser beam into the interferometer as plotted in Fig. 3, and obtained the spiral interference pattern as given in Fig. 5(g). This left handedness of the spiral fringe proved that the topological charge of laser beam didn't change and remained to be −1 when it was switched from radial polarization to azimuthal polarization.

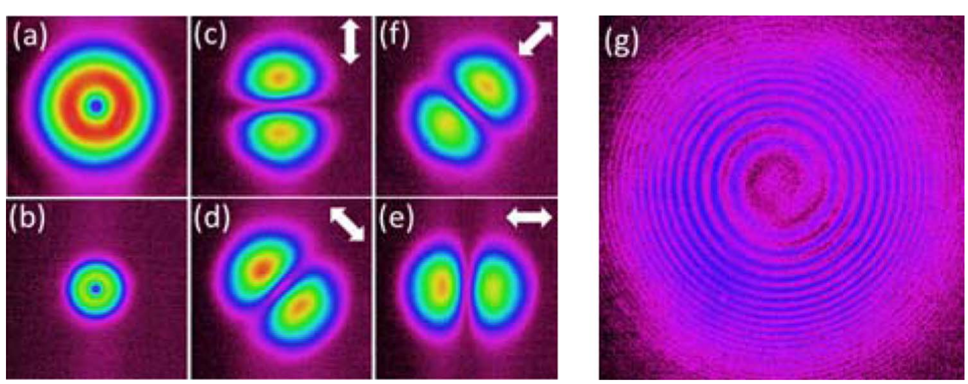

Fig. 4. (a) Far- and (b) near-field intensity distributions of the laser beam at $P_{\text{abs}} = 3.8$ W for passively Q-switched Nd:YAG laser; (c)–(f) variations of far-field intensity distribution of the passage beam through the polarizer analyzer with different orientations of the polarizer axes (where white arrows indict the directions of the polarizer analyzer's axis); (g) measured interference pattern.

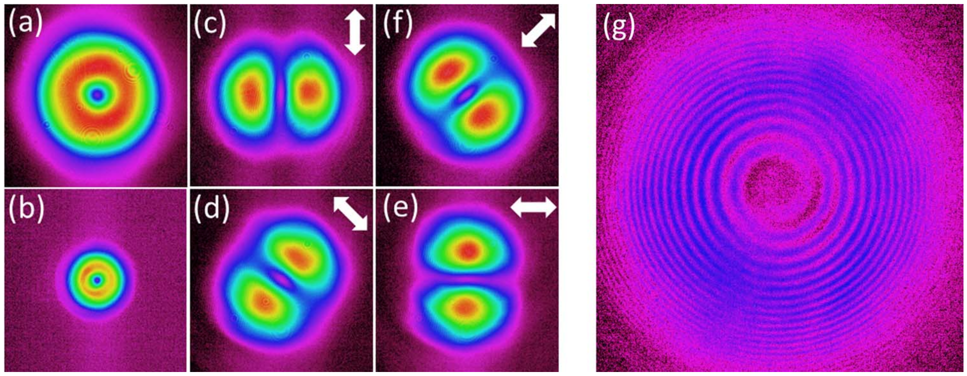

Fig. 5. (a) Far- and (b) near-field intensity distributions of the laser beam; (c)–(f) variations of far-field intensity distribution of the passage beam through the polarizer analyzer with different orientations of the polarizer axes (where white arrows indict the directions of the polarizer analyzer's axis); (g) measured spiral interference pattern with left handedness.

In conclusion, we demonstrate the utilization of an active resonator to emit vector beam with helical wavefront. The laser is compact with simple plano–plano cavity configuration. For CW operation, this laser emits radially polarized beam, and the helical wavefront of it can be transformed from right handedness to left handedness by tilting the OC. For passively Q-switched operation, both the radially and azimuthally polarized LG_{01} modes are obtained with the left-handedness helical wavefront. The spiral phase structure incorporated in vector laser beam will facilitate many applications.

References

1. M. R. Dennis, K. O. Holleran, and M. J. Padgett, "Singular optics: optical vortices and polarization singularities," in *Progress in Optics*, E. Wolf, ed. (Elsevier, 2009), Vol. **53**, p. 294.
2. D. L. Andrews, *Structured Light and its Applications: An Introduction to Phase-Structured Beams and Nanoscale Optical Forces* (Elsevier, 2008).
3. L. Allen, M. W. Beijersbergen, R. J. C. Spreeuw, and J. P. Woerdman, Phys. Rev. A **45**, 8185 (1992).
4. Y. Yao, K. Xia, M. Kang, Z. Fang, and J. Li, Chin. Opt. Lett. **11**, 121406 (2013).
5. J. J. Yu, C. H. Zhou, W. Jia, A. D. Hu, W. G. Cao, J. Wu, and S. Q. Wang, Appl. Opt. **51**, 6799 (2012).
6. B. Terhalle, A. Langner, B. Päivänranta, V. A. Guzenko, C. David, and Y. Ekinci, Opt. Lett. **36**, 4143 (2011).
7. J. Chen, Y. Yu, and F. Wang, Chin. Opt. Lett. **9**, 011402 (2011).
8. Q. W. Zhan, Adv. Opt. Photon. **1**, 1 (2009).
9. R. Oron, S. Blit, N. Davidson, A. A. Friesem, Z. Bomzon, and E. Hasman, Appl. Phys. Lett. **77**, 3322 (2000).
10. Y. Kozawa and S. Sato, Opt. Lett. **30**, 3063 (2005).
11. K. Yonezawa, Y. Kozawa, and S. Sato, Opt. Lett. **31**, 2151 (2006).
12. K. Otsuka and S. C. Chu, Opt. Lett. **38**, 1434 (2013).
13. J. L. Li, K. Ueda, M. Musha, L. X. Zhong, and A. Shirakawa, Opt. Lett. **33**, 2686 (2008).
14. D. Lin, K. G. Xia, J. L. Li, R. X. Li, K. Ueda, G. Q. Li, and X. J. Li, Opt. Lett. **35**, 2290 (2010).
15. Z. M. Zhang, J. X. Pu, and X. Q. Wang, Appl. Opt. **47**, 1963 (2008).
16. Z. Y. Chen and D. M. Zhao, Opt. Lett. **37**, 1286 (2012).
17. L. N. Guo, Z. L. Tang, Y. B. Wu, and C. Q. Liang, Eur. Phys. J. Appl. Phys. **62**, 31101 (2013).
18. D. G. Grier, Nature **424**, 810 (2003).
19. J. Ng, Z. F. Lin, and C. T. Chan, Phys. Rev. Lett. **104**, 103601 (2010).
20. L. Huang, H. L. Guo, J. F. Li, L. Ling, B. H. Feng, and Z. Y. Li, Opt. Lett. **37**, 1694 (2012).
21. W. J. Gu, Z. H. Zhou, and Q. F. Tan, Proc. SPIE **8202**, 82020W (2011).
22. J. Allegre, W. Perrie, S. P. Edwardson, G. Dearden, and K. G. Watkins, J. Opt. **14**, 085601 (2012).
23. Z. Bomzon, V. Kleiner, and E. Hasman, Opt. Lett. **26**, 1424 (2001).
24. G. Biener, A. Niv, V. Kleiner, and E. Hasman, Opt. Lett. **27**, 1875 (2002).
25. M. Beresna, M. Gecevičius, P. G. Kazansky, and T. Gertus, Appl. Phys. Lett. **98**, 201101 (2011).
26. Z. Q. Fang, Y. Yao, K. G. Xia, M. Q. Kang, K. Ueda, and J. L. Li, Opt. Commun. **294**, 177 (2013).
27. Z. Q. Fang, K. G. Xia, Y. Yao, and J. L. Li, Appl. Phys. B **117**, 219 (2014).
28. Z. Q. Fang, K. G. Xia, Y. Yao, and J. L. Li, IEEE J. Sel. Top. Quantum Electron. **21**, 1 (2015).